

Sediment consolidation settlement of Chengbei Sea area in the northern Huanghe River subaqueous delta, China*

LIU Jie (刘杰)^{1,2}, FENG Xiuli (冯秀丽)^{2,3,**}, LIU Xiao (刘潇)^{2,4}

¹ Key Laboratory of Marine Sedimentology and Environmental Geology, First Institute of Oceanography, State Oceanic Administration (SOA), Qingdao 266061, China

² Laboratory for Marine Geology, Qingdao National Laboratory for Marine Science and Technology, Qingdao 266061, China

³ Key Lab of Submarine Geosciences and Prospecting Techniques, Ocean University of China, Qingdao 266100, China

⁴ College of Environmental Science and Engineering, Ocean University of China, Qingdao 266100, China

Received Dec. 30, 2015; accepted in principle Feb. 23, 2016; accepted for publication Apr. 8, 2016

© Chinese Society for Oceanology and Limnology, Science Press, and Springer-Verlag Berlin Heidelberg 2017

Abstract One of the most important factors controlling the morphology of the modern Huanghe (Yellow) River delta is consolidation settlement, which is impacted by fast deposition, high water content, and low density of seafloor sediment. Consolidation settlement of the Huanghe River subaqueous delta was studied based on field data, laboratory experiments on 12 drill holes, and the one-dimensional consolidation theory. Results show that vertical sediment characteristics varied greatly in the rapidly forming sedimentary bodies of the modern Huanghe River subaqueous delta. Sediments in the upper parts of drill holes were coarser than those in the deeper parts, and other physical and mechanical properties changed accordingly. On the basis of the one-dimensional consolidation theory and drilling depth, the final consolidation settlement of drill holes was between 0.6 m and 2.8 m, and the mean settlement of unit depth was at 1.5–3.5 cm/m. It takes about 15–20 years for the consolidation degree to reach 90% and the average sedimentation rate within the overlying 50 m strata was at 5 cm/a to 12 cm/a. This study helps to forecast the final consolidation settlement and settlement rate of the modern Huanghe River subaqueous delta, which provides key geotechnical information for marine engineers.

Keyword: mechanical properties; consolidation settlement; drill hole; modern Huanghe River subaqueous delta

1 INTRODUCTION

The modern Huanghe (Yellow) River delta is the largest and youngest wetland in China. In recent years, research on the Huanghe River delta was mostly focused on river discharge, sediment input, changes of the river channel, and coastal erosion (Liu et al., 2001, 2002; Wang et al., 2001; Feng et al., 2004; Guan and Gu, 2011). Studies of the Huanghe River delta erosion were based on water depth measurement (Chu et al., 2005), but the delta morphology is controlled by a variety of factors, including suspended sediment load, coastal engineering, hydrodynamic environment, and consolidation settlement.

Land subsidence of the Huanghe River delta has been caused by three major factors. The first is neotectonics and global sea-level rise (Liu et al., 2011).

Second, consolidation and compaction has occurred as a result of subsidence of imbricate delta lobes (Bie et al., 2006). The initial consolidation settlement rate was relatively high and decreased over time. Third, the Huanghe River delta comprises numerous funnel shaped lobes, which formed over time. Many of these lobes formed owing to human intervention and activities (Qin et al., 2008). Of these, the most important factor for land subsidence in the Huanghe River subaqueous delta was natural consolidation and compaction.

* Supported by the National Science Foundation for Young Scientists of China (No. 41206054), the Joint Fund of the National Natural Science Foundation of China and Shandong Province (No. U1606401), and the Special Fund of Chinese Central Government for Basic Scientific Research Operations in Commonweal Research Institutes (No. 2015G08)

** Corresponding author: fengxiuli@ouc.edu.cn

To date, research on subsidence has mainly concentrated on land area. Land subsidence has been monitored from 1891 in Mexico City, and the largest cumulative settlement was above 7.5 m (Ortega-Guerrero et al., 1999). Land subsidence also had been found in 1898 in Niigata, Japan, and the maximum subsidence rate was at 53 cm/a in 1958 (Miura et al., 1988). Monitoring of land subsidence in China has been expanded to the Changjiang (Yangtze) River delta and Huanghe River-Huaihe-Haihe Plain (Xue et al., 2003). Land subsidence monitoring methods of land subsidence mainly include regional geodetic leveling (Teatini et al., 2005), permanent scatterers interferometry (Meisina et al., 2006), Global Positioning System technique data (Gili et al., 2000), Geographic Information System techniques (Su et al., 2010), Differential Interferometric Synthetic Aperture Radar (D-InSAR) techniques (Wu et al., 2004; Fan et al., 2011), and Persistent Scatterers InSAR techniques (Parcharidis et al., 2009; Tung and Hu, 2012).

Chinese and international research has focused on subsidence in land areas of the modern Huanghe River delta (Hu et al., 2004; Jiang and Lin, 2010). Research on the subaqueous delta was mostly focused on sediment input, coastline erosion, and erosion and deposition of the seabed. Studies of consolidation settlement in the subaqueous delta are limited. In this paper, consolidation settlement of the modern Huanghe River subaqueous delta was studied based on drilling data and laboratory experiment results. Final consolidation settlement amounts and settlement rates were forecasted, to minimize the impacts from geological hazards caused by consolidation settlement and to provide important parameters for marine engineering.

2 STUDY AREA

2.1 Modern Huanghe River delta

The modern delta began forming in 1855 when a major channel adjustment took place at Tongwaxiang, and most suspended load of the Huanghe River began to deposit within the modern active delta in the Bohai Sea. The modern Huanghe River delta is one of the youngest deltas in the world (Bie, 2006). The modern Huanghe River delta is rich in oil and gas resources and has great significance to China's energy supply and economic development. The modern delta is composed of juxtaposed and imbricate deltaic lobes, which formed around the mouth of the river at different times (Shi et al., 2003). Since 1855, eight

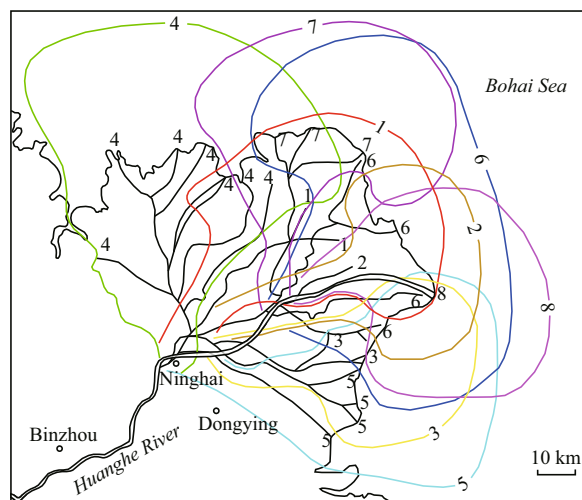


Fig.1 Lobes of the modern Huanghe River delta

1. 1855–1889; 2. 1889–1897; 3. 1897–1904; 4. 1904–1929; 5. 1929–1934; 6. 1934–1964; 7. 1964–1976; 8. 1976–1994) (Xue, 1994).

deltaic lobes have formed (Fig.1), and the average duration of the channel belt and mouth bar deposition in each lobe was about 18 years (Xue, 1994). Statistic data of Huanghe River Conservancy Commission of Ministry of Water Resources (MWR) indicate the mean annual suspended sediment load in the past 60 years was about 7.22×10^8 ton/a. Annual runoff and suspended sediment load have decreased over time owing to the construction of upstream reservoirs and water-sediment regulation experiments. Mean suspended sediment load at the Lijin station was 3.13×10^8 ton/a between 1988 and 2009, and only 1.05×10^8 ton/a between 2010 and 2012 (Huanghe River Conservancy Commission of MWR, 1951–2012).

2.2 Natural environment

The modern Huanghe River delta, located on the west coast of Laizhou Bay and the south coast of the Bohai Bay, is under the influence of a subhumid warm monsoon climate. The average annual temperature is 12.8°C , and the average annual rainfall is 613.6 mm. The modern Huanghe River subaqueous delta can be divided into three components: 1) topset-delta plain (water depth of 0–3 m; slope of 0.01° – 0.03° ; width of 7–8 km); 2) foreslope (water depth of 3–14.5 m; slope of 0.25° – 0.35° ; width of 5–7.5 km); 3) prodelta (water depth greater than 14.5 m; slope of 0.01° – 0.03° ; width of 4.5–8 km) (Yang et al., 1990). Offshore region of the study area is mainly mixed semidiurnal tides with flood duration lower than ebb duration. The average flow velocity of flood tide is 38 cm/s at the surface and 30 cm/s at the bottom, and the ebb tide

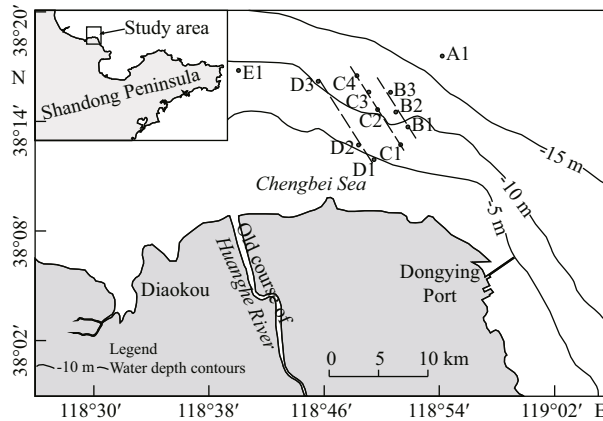


Fig.2 Position of study area and drill holes

flow velocity is lower than that of the flood tide (Cui et al., 2001). The direction of normal wave in the study area is northeast, which is mainly controlled by wind, and the frequency is 10.3% (Ren and Chen, 2012).

3 MATERIAL AND METHOD

3.1 Data sources

In this paper, engineering geological investigation data, laboratory analysis data, stratigraphic profiles, and analysis reports from the year 2000 of Chengbei sea area in the Huanghe River subaqueous delta were collected to study the vertical distribution characteristics of sediments and the geotechnical engineering properties of different settled layers, and calculate the consolidation settlement amount and rate of each drill hole. The locations of the study area and the cores are shown in Fig.2.

3.2 Method

3.2.1 Calculation of the final settlement

Physical properties and effective stresses varied in different layers owing to different depositional environments. The final consolidation settlement of the settled layers in the subaqueous delta was calculated by the layerwise summation method and Terzaghi's one-dimensional consolidation theory (Terzaghi, 1943). Each settled layer should meet the following three hypotheses: 1) the settled layer is homogeneous, and the soil particles and pore water are incompressible; 2) compression of the soil should meet the compress law; 3) pore water infiltration occurred in the vertical direction, and must obey Darcy's law (Swartzendruber, 1962; Hansbo, 2003).

Each of the studied drill holes were divided into several layers based on drilling data, sediment grain size, and physical properties to calculate the final settlement. Consolidation settlement of a layer i can be expressed as follows:

$$\Delta s_i = \frac{e_{1i} - e_{2i}}{1 + e_{1i}} h_i, \quad (1)$$

where Δs_i is the compression deformation of the settled layer (m); h_i is the thickness of the settled layer (m); e_{1i} is the void ratio of the undisturbed soil mass; and e_{2i} is the void ratio of stable conditions under the effect of gravity stress and additional stress.

And

$$a_i = -\frac{e_{2i} - e_{1i}}{p_{2i} - p_{1i}}, \quad (2)$$

where a_i is the coefficient of compressibility in the studied settled layer (/kPa); p_{1i} is the geostatic stress of the studied settled layer (kPa); and p_{2i} is the sum of gravity stress and additional stress (kPa).

Thus, the final settlement of the drill hole is as follows:

$$s = \sum_{i=1}^n \Delta s_i = \sum_{i=1}^n \frac{a_i (p_{2i} - p_{1i})}{1 + e_{1i}} h_i. \quad (3)$$

3.2.2 Calculation of the consolidation degree

Consolidation settlement and consolidation degree were different in different layers within a certain period of time because of different physical properties and effective stresses. The layerwise summation method was also used in the calculation of consolidation degree, to obtain the consolidation degree in different layers within a certain time:

$$U = \frac{s_t}{s} = 1 - \frac{8}{\pi^2} \sum_{n=1}^{\infty} \frac{1}{(2n+1)^2} \exp \left[-\left(\frac{2n+1}{2} \pi \right)^2 T_v \right]. \quad (4)$$

And

$$T_v = \frac{C_v}{H^2} t, \quad (5)$$

$$C_v = \frac{k(1 + e_1)}{\gamma_w \cdot a}, \quad (6)$$

where n is a positive odd number (1, 3, 5, ...); T_v is the time factor; C_v is the consolidation coefficient of the settled layer (cm^2/a); H is the thickness of the settled layer (m); t is the elapsed time of consolidation settlement (a); k is the osmotic coefficient (cm/a); e_1 is the void ratio of the undisturbed settled layer; γ_w is the unit weight of waters (kN/m^3); and a is the coefficient of compressibility (/MPa).

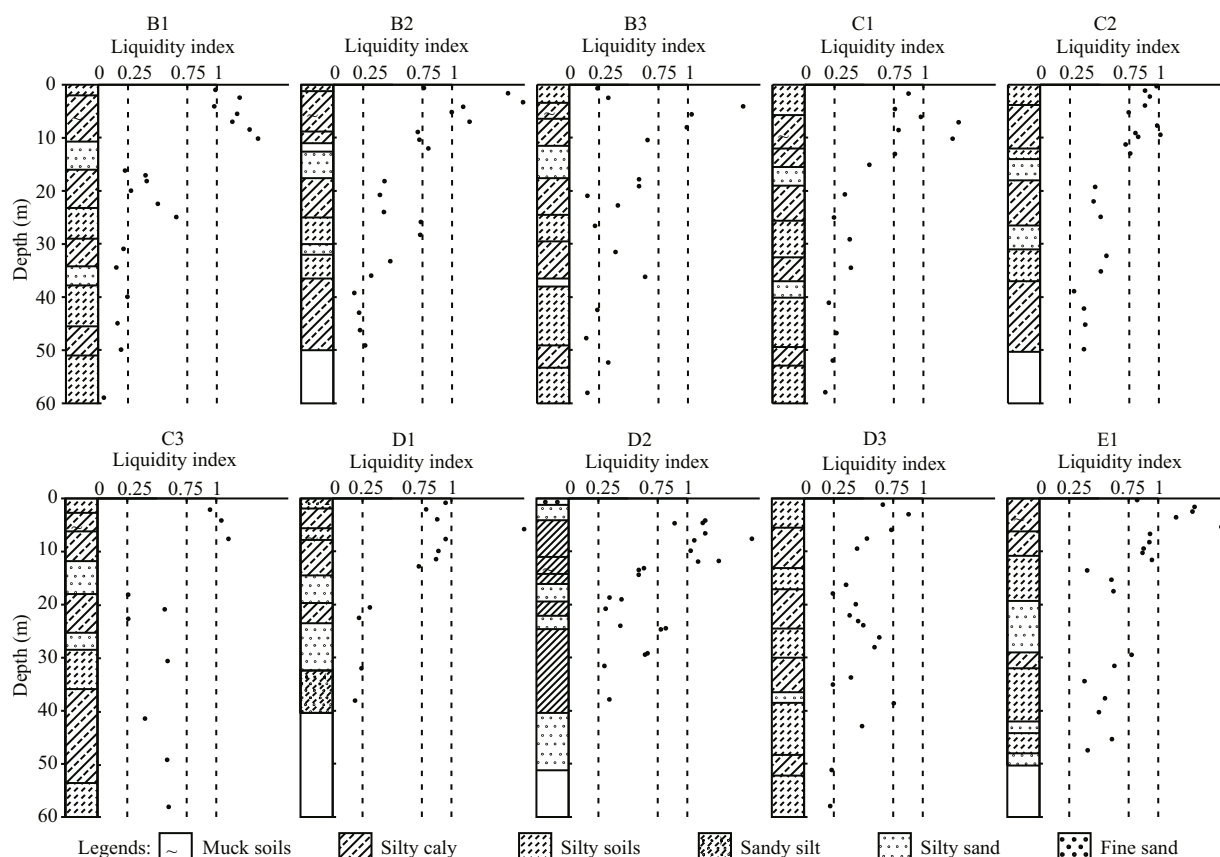


Fig.3 Vertical distribution of liquidity index and sediment types of cores in the study area

Differences in the permeability coefficient in different strata had an important influence on the variation rate of sediment consolidation settlement, while it made no difference on the amount of the final consolidation settlement. The consolidation process needed relatively short time to reach steady state because the permeability coefficient was large. In addition, it was characterized by erosion in the study area, with only a small scope of siltation in the north side of the study area. Influence of topographical change on sediment consolidation settlement was mainly focused on the overlying effective stresses. In this paper, the overlying effective stress used in the calculation left out a consideration of erosion and deposition over time, owing to small deposition-erosion variation and lack of observed water depth data.

4 RESULT

4.1 Vertical distribution of sediment characteristics

The drill holes in the study area were located near the old course of the modern Huanghe River estuary, and variation of sediment characteristics and

geotechnical engineering mechanical properties in depth were roughly the same owing to the same large scale sedimentary environment. For example, the liquidity index decreased gradually from the surface to the bottom in all drill holes. Sediments above 10 m in depth were in a flexible plastic-flow plastic state, and the liquidity index was above 0.75. The sediments were in a plastic state between 10 m and 40 m, and were in a hard plastic state below 40 m. These characteristics support the interpretation that the sediments above 10 m were modern delta and Holocene neritic deposits with high compressibility.

The 12 drill holes can be broadly divided into 7 to 13 layers based on field notes, particle size and laboratory geotechnical analyses (Fig.3). The sediments are mainly silty clay and silt, containing some sandy silt, silty sand, and fine sand, based on the Code for Design of Building Foundation (GB50007-2011) promulgated by the Ministry of Housing and Urban-rural Development of the People's Republic of China in 2011. Vertical distribution of sediment characteristics was roughly the same: surface sediments were silty soils, and sludge under the surface sediments within the upper 10 m. The silty

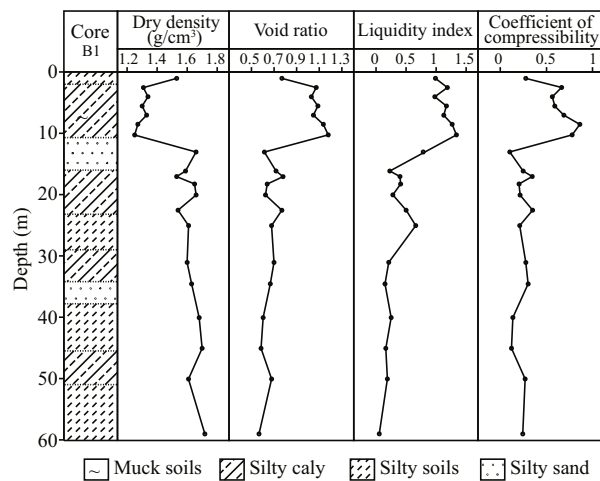


Fig.4 Dry density, void ratio, liquidity index and compressibility of drill hole B1

clay and silt appeared alternately in the underlayer, with occasionally some fine sand, sandy silt and silty sand.

As the vertical distributions of geotechnical engineering mechanical properties and sediment characteristics of different drill holes were similar, drill hole B1 was taken for example to analyze the sedimentary environment and engineering properties of different layers (Fig.4). The drill hole was divided into 6 layers and 10 sublayers based on field notes, particle size, and geotechnical analysis data, referring to shallow stratigraphy profiles (Geopulse subbottom profiler, resolution ratio 1 m, England) and extremely shallow stratigraphy profiles (SBP-5000 subbottom profiler, resolution ratio 0.2 m, USA). Compared with previous research on sediment dating, grain size parameters, and sedimentary environment stratification in different drill holes of the modern Huanghe River supaqueous delta (Zhuang et al., 1999; Li et al., 2013) and subaqueous delta near the study area (Liu et al., 2009), sedimentary environments and geotechnical engineering properties of different layers can be summarized as follows:

Unit 1 (0 m to -2 m) is a fluvial-dominated delta facies mainly controlled by river transport. After the diversion of the Huanghe River estuary, the delta lobe began to erode under the action of hydrodynamic forces. In this process, finer superficial sediment particles were taken away, and the coarser particles were retained. Thus, the sediment of Unit 1 is mainly composed of silt and can be liquefied by earthquake and storm waves.

Unit 2 (-2 m to -10.7 m) is delta and tidal flat facies, -2 m to -6.8 m is delta sediment carried by the

Huanghe River after 1855 and the lower part is tidal flat sediment formed before 1855. This unit is mainly composed of mucky silty clay with a high void ratio, high compression coefficient, and high liquidity index.

Unit 3 (-10.7 m to -16 m) is the Holocene fluviolacustrine facies. About 8 800 years ago, the study area underwent a large scale transgression (Huanghua, 9000–0 yr B.P.), and gradually evolved into a tidal flat, coastal and shallow marine environment. The lower bound of this unit is the planation surface of the Huanghua Holocene marine intrusion. The sediment of Unit 3 is silt with good sorting and medium compressibility.

Unit 4 (-16 m to -29 m) contains two parts. The upper part (-16 m to -23.2 m) is continental deposits that correspond to the glacial period at the end of the Pleistocene. The lower part (-23.2 m to -29 m) is marine deposits formed during the Xianxian transgression (39 000–22 000 yr B.P.). The upper and lower sediment of Unit 4 is plastic or hard plastic silty clay and plastic, medium compressible silt, respectively.

Unit 5 (-29 m to -51 m) is characterized by a long time span and complex depositional environment, which consists of Late Pleistocene alternating continental and marine layers. This Unit can be divided into four sublayers from top to bottom. The first sublayer is plastic or hard plastic transitional silty clay with a thickness of 5.2 m. The second sublayer, from -34.2 m to -37.8 m, is a thin layer of littoral deposits composed of well-sorted silt. The third sublayer (-37.8 m to -45.5 m) is high-strength silt with few clay particles showing the characteristics of continental sedimentation. The fourth sublayer (-45.5 m to -51 m) is silty clay of marine facies.

Unit 6 (-51 m to -60.1 m, did not reach the bottom) is composed of hard plastic silt from continental deposits of the early Late Pleistocene.

The sediments above 60 m in the study area are consisted of Late Pleistocene and Holocene deposits in alternating continental and marine layers. Under the effect of marine hydrodynamics, surface sediments is obviously coarser than lower sediments. The sediment above -10.7 m is rapidly formed delta deposits and Holocene neritic deposits, and consists mainly of under-consolidated soft soil. Except for the surface silt layer, the drilling samples consist of low-strength soil with medium to high compressibility, and the soil strength generally increases from top to bottom.

Table 1 Physical and mechanical properties and final settlement of drill hole A1

Layer number	Sediment types	Layer thickness (m)	Void ratio	compressibility index (/Mpa)	Effective unit weight (kN/m ³)	Settlement (cm)
1	Silty clay	6.6	1.530	0.819	7.5	5.29
2	Silty clay	2.7	0.891	0.379	9.3	3.36
3	Silty soils	1.2	0.735	0.231	9.8	1.29
4	Silty sand	4.2	0.676	0.132	10.0	3.55
5	Clay	2	0.831	0.253	9.4	3.81
6	Fine sand	2.5	0.607	0.116	10.1	2.88
7	Silty clay	4.3	0.729	0.265	9.9	12.77
8	Silty soils	7.1	0.668	0.219	10.0	26.66
9	Silty clay	6.6	0.715	0.232	9.9	28.45
10	Silty soils	3.3	0.663	0.189	10.0	13.80
11	Silty sand	5.3	0.617	0.136	10.1	18.33
12	Fine sand	11.7	0.573	0.093	10.4	34.50
13	Silty soils	3	0.654	0.099	10.1	10.32

4.2 Final consolidation settlement

The calculation of consolidation settlement was stated with normal consolidation and under consolidated condition because no up loading occurred in the modern Huanghe River subaqueous delta. The final consolidation settlement of drill hole A1, for example, was calculated by one-dimensional consolidation theory and layerwise summation method. The final settlement of each layer caused by different geotechnical engineering properties, sediment types, and overburden pressures at depth is shown in Table 1.

According to the calculated results, 60 m of depth could produce a total of 1.65 m settlement in drill hole A1. The plotted subsidence curve based on soil subsidence of each layer can be divided into three sections. The sediments above 10 m are delta and Holocene neritic deposits with high compressibility and no imposed load, and the sediments between 10 and 20 m are silt and fine sand with low compressibility. The consolidation settlement of section one is not significant, and the consolidation settlement of unit depth is about 1.1 cm/m. The second section makes the most significant contribution to the final consolidation settlement owing to suitable geotechnical engineering properties and the overburden pressure of silty clay. The final settlement is 0.82 m within the 21.3 m section, and the settlement of unit depth is about 3.9 cm/m. The third section is composed of silt and fine sand with low compressibility, while the final settlement is still large owing to high overburden pressure. The depth of the section is 20 m

and the final settlement is 0.63 m, and the consolidation settlement of unit depth is about 3.1 cm/m.

The final settlements of different layers in each drill hole caused by diverse geotechnical engineering properties and overburden pressures at depth are shown in Table 2, and their subsidence curves have been plotted (Fig.5). As can be seen in the figure, the final consolidation settlement of each drill hole is between 0.6 m and 2.8 m, and the settlement of unit depth is at 1.5–3.5 cm/m. These ranges are probably due to different drilling depth, sedimentary environment, composition of sediments, consolidation time, physical and mechanical property, and etc. The curves can be divided into three types based on different settlement of unit depth in vertical: 1) settlement of unit depth was large in the middle and small at the surface and bottom of drill holes A1, C3, and D2; 2) settlement of unit depth was relatively constant in depth, and the representative drill holes were D1, D3, and E1; 3) settlement of unit depth gradually increased from the surface to the bottom in drill holes B1, B2, B3, C1, C2, and C4.

4.3 Changes of consolidation degree over time

All of the analyses in this paper were based on collected data, and some drill holes were short of permeability coefficient data. Drill holes B1 and C1 were collected with complete experimental data to study consolidation degree and changes of sedimentation rates over time (years of 1st, 2nd, 3rd, 5th, 10th, 15th, and 20th) based on physical and mechanical data for each layer. The consolidation settlement

Table 2 Stratification, compressibility index and final settlement of drill holes in the study area

Core	B1			B2			B3			C1		
No.	d	a_{1-2}	C_s	d	a_{1-2}	C_s	d	a_{1-2}	C_s	d	a_{1-2}	C_s
1	2.0	0.28	0.3	1.2	0.19	0.1	3.4	0.10	0.4	5.7	0.25	2.4
2	8.7	0.69	15.7	7.6	0.66	9.2	3.0	0.77	4.7	6.3	1.05	26.0
3	5.3	0.10	3.9	3.0	0.45	6.1	5.1	0.52	10.9	3.5	0.49	12.1
4	7.2	0.27	20.8	1.6	0.17	1.7	6.1	0.12	5.9	3.5	0.26	8.7
5	5.8	0.21	17.8	5.0	0.10	4.4	6.9	0.27	21.5	6.6	0.26	21.6
6	5.2	0.28	25.6	7.4	0.29	24.9	5.0	0.28	22.1	6.9	0.28	33.9
7	3.6	0.30	22.7	5.0	0.20	15.8	7.0	0.32	38.8	4.6	0.28	26.5
8	7.7	0.13	27.5	2.0	0.01	0.4	1.5	-	0.0	3.1	-	0.0
9	5.5	0.27	42.0	4.5	0.06	5.5	11.1	0.11	32.5	9.3	0.21	54.3
10	9.1	0.24	77.4	13.5	0.21	70.0	4.2	0.34	40.3	3.5	0.32	34.8
11	-	-	-	-	-	-	7.2	0.12	30.8	7.3	0.19	51.6
Sum	60.1	-	253.7	50.8	-	138.0	60.5	-	207.9	60.3	-	272.0
Core	C2			C3			C4			D1		
No.	d	a_{1-2}	C_s	d	a_{1-2}	C_s	d	a_{1-2}	C_s	d	a_{1-2}	C_s
1	3.8	0.22	0.9	2.7	0.12	0.2	2.6	0.12	0.2	1.9	0.17	0.2
2	8.2	0.49	15.9	3.5	0.81	5.1	8.9	0.42	14.0	3.7	0.39	2.6
3	2.0	0.25	3.6	5.6	0.49	11.2	6.1	0.18	9.6	1.8	0.88	3.9
4	4.0	0.12	4.3	6.2	0.26	12.3	6.4	0.17	13.4	3.8	0.44	6.8
5	8.5	0.26	26.4	7.3	0.34	27.6	5.5	-	0.0	2.9	0.33	5.7
6	4.5	0.01	0.8	3.2	-	0.0	6.5	0.24	30.2	5.2	0.12	5.6
7	6.0	0.13	15.5	7.4	0.15	20.3	16.5	0.24	97.9	3.8	0.17	7.2
8	13.3	0.22	81.5	17.7	0.33	172.6	7.7	0.25	69.0	8.9	0.09	14.3
9	-	-	-	6.9	0.13	18.8	-	-	-	8.0	0.09	15.3
Sum	50.3	-	148.9	60.5	-	268.2	60.2	-	234.4	40.0	-	61.6
Core	D2			D3			E1					
No.	d	a_{1-2}	C_s	d	a_{1-2}	C_s	d	a_{1-2}	C_s			
1	4.1	0.08	0.4	5.5	0.14	1.2	6.2	1.01	6.2			
2	1.6	0.48	1.9	7.6	0.55	21.1	4.6	0.49	7.6			
3	3.0	0.64	6.1	4.0	0.19	7.4	8.5	0.36	24.1			
4	1.3	0.70	3.8	7.4	0.21	18.6	9.7	0.17	23.0			
5	3.2	0.89	13.9	5.5	0.15	13.6	3.0	0.30	14.7			
6	1.9	0.16	2.5	6.5	0.22	27.0	10.0	0.23	46.7			
7	3.3	0.08	2.9	2.0	-	0.0	2.2	0.09	5.0			
8	2.7	0.24	8.2	9.8	0.13	38.1	3.8	0.22	22.1			
9	2.5	-	0.0	3.9	0.22	24.9	2.3	0.10	6.6			
10	8.4	0.25	33.4	8.0	0.12	32.5	-	-	-			
11	7.4	0.25	38.8	-	-	-	-	-	-			
12	10.8	0.08	24.0	-	-	-	-	-	-			
Sum	50.2	-	135.9	60.2	-	184.5	50.3	-	156.1			

Note: d : thickness of sediments (m); a_{1-2} : compressibility index (/Mpa); C_s : final consolidation settlement (cm).

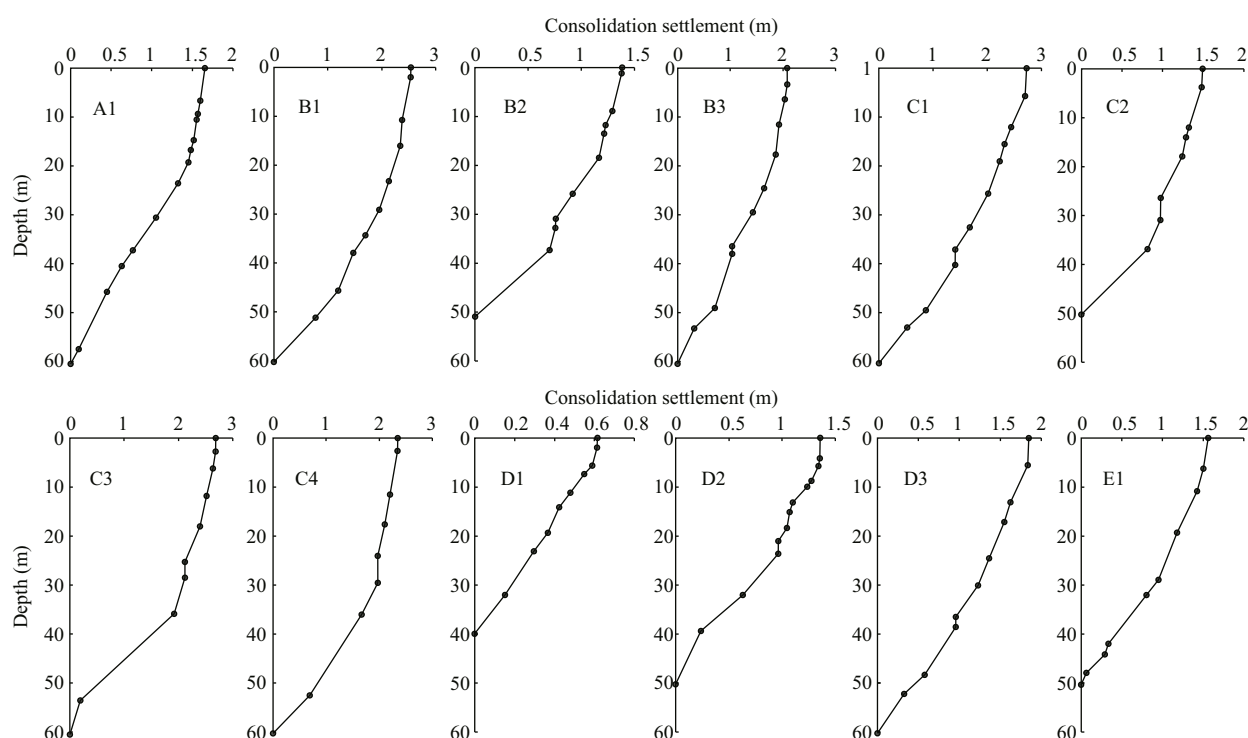


Fig.5 Subsidence curves and final settlement of each core

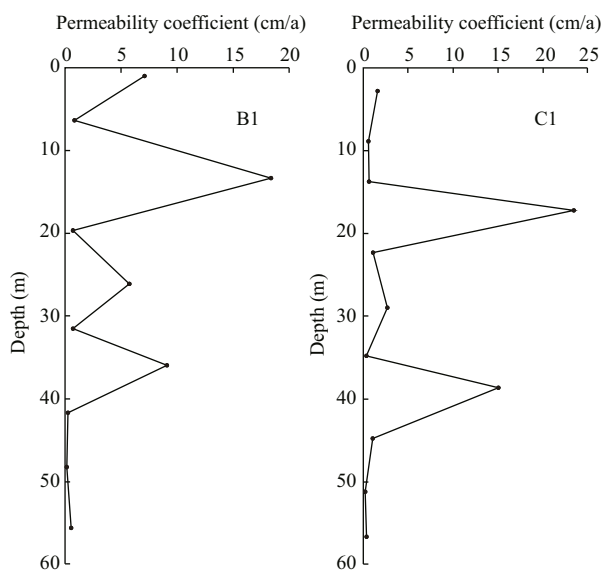


Fig.6 Changes of the permeability coefficient curves along depth

process was controlled by the coefficient of permeability, while compressibility and void ratios varied with time and effective stress. The average values of the factors were taken to simplify the calculations. The permeability coefficient curves are shown in Fig.6 and the results of changes of consolidation degree over time are shown in Fig.7.

Consolidation degree increased with the increase of time, although the rate decreased with time. The

fastest consolidation occurred in the first 5 years during which time the consolidation degree could reach 60% to 70%, while to reach 90% from 80% also took approximately 5 years. In general, the consolidation degree needed 15–20 years to reach 90%, and the average sedimentation rate was 5 cm/a to 12 cm/a within the study area.

5 DISCUSSION

5.1 Consolidation of the delta near the current estuary

In the study area, sediments above 10 m are delta and Holocene neritic deposits with high water content, high void ratio, and high liquidity. These deposits are high compressibility soil, but because they have no imposed load, their consolidation settlement is not significant.

The distance between the study area and the modern Huanghe River subaqueous delta is short, and the geotechnical engineering properties in depth are mostly similar for the two locations. Assuming that the delta in the study area formed above the sea level, the consolidation settlement of high compressibility sediments above 10 m is greater owing to the greater overburden stress. For example, at drill hole A1, the water depth is -10 m, supposing that the seabed was higher than the sea level; the effective density of the

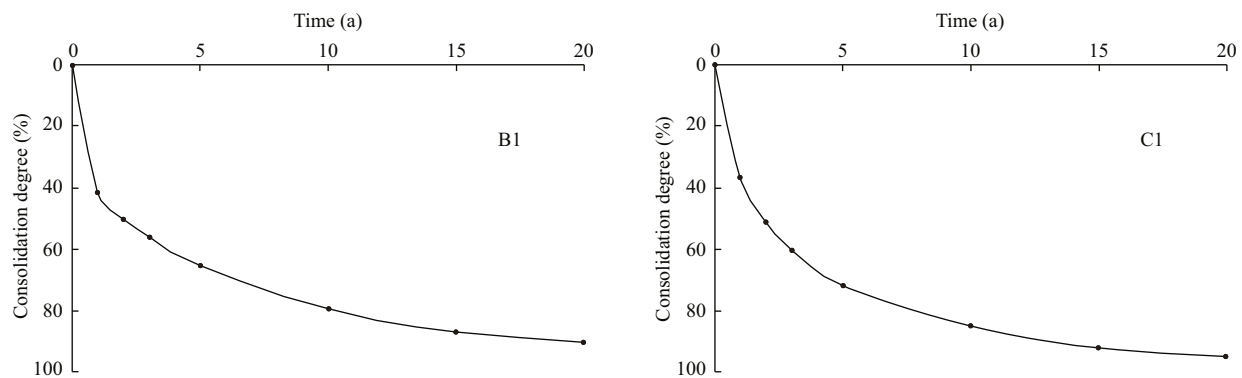


Fig.7 Changes of consolidation degree versus time for drill holes B1 and C1

overlying soil layer was 10 kN/m^3 ; and the other conditions remained invariant. The final consolidation settlement within the above 10 m increased from 10 cm to 38.3 cm. The consolidation settlement had a significant effect on submarine topography changes in the current estuary of the Huanghe River, with feature of high sediment input.

5.2 Vertical distribution of sediment characteristics

Vertical distribution of sediment types and geological engineering characteristics of each drill hole was studied. Surface sediments were composed of coarse silt with high intensity, while the layer immediately below the surface layer was composed of mud with high water content, high void ratio, and high liquidity. This is mainly because the modern Huanghe River subaqueous delta formed in the study area and adjacent waters, and the delta began to erode after the diversion of the Huanghe River estuary. The clay and other fine particulate materials of delta deposits in the upper strata were carried away under the effect of hydrodynamic force. Relatively coarse sediments were retained, while the underlying mud layer was basically unchanged.

5.3 Consolidation settlement rate

The consolidation settlement rate tapered off over time as no more sediment accumulation. As shown in Fig.7, the consolidation degree needed about 20 years to reach 90%; it could reach 60% within the first 5 years, while about 10 years was needed to reach 90% from 80%. This was mainly because the sediments were composed of silt and silty clay. The consolidation degree could reach 90% within 1 year in the settled layer of silt, owing to its high osmotic coefficient and fast consolidation rate. In addition, osmotic coefficient, coefficient of compressibility, and void ratio decreased with the settlement of the settled layer.

5.4 Settlement contribution of different layers

The final consolidation settlement was controlled by overburden pressure, physical and mechanical properties. Changes of these factors would influence the contribution of consolidation settlement. The settlement characteristics of the drill holes were comparable and all of them could be divided into three sections. The sediment of the first section is delta and Holocene neritic deposits with high void ratio, liquidity index, and compressibility. Settlement in the first section was minimal because sediments were under their own average gravity stress, with no overburden pressure. The consolidation settlement contribution in the second and third section varied in different holes. Under the same overburden pressure, the final settlement was controlled by the sediment types, physical and mechanical properties. Clay and other fine particulate materials with high void ratio and compressibility would produce large settlement, while coarse sediments such as silt and sand with low compressibility would produce small settlement.

5.5 Implications of the results

Sediments of the modern Huanghe River delta have features of high water content, high void ratio, high sensitivity and low capacity owing to rapid accumulation, and are easily liquefied under wave effects. According to the results of this study, surface sediments become coarser and form a hard layer under wave loading in the Chengbei Sea area, where there are no sediment sources after the diversion of the Huanghe River. However, sediments of the modern Huanghe River still have features of high water content, high liquidity index, and high compressibility, but no hard layer on the surface. Thus, if sea walls, jetties, levees, or groins are to be constructed in the modern Huanghe River deltaic

coast, consolidation settlement characteristics of sediments under self-weight pressure and effective overburden pressure should be considered preferentially. The settlement amount and characteristics under the pressure of marine structures, and the design elevation of those structures can be understood through theoretical calculation or numerical simulation.

These results can offer a scientific basis for the economic design and safe operation of ocean engineering in the modern Huanghe River subaqueous delta, and provide a geological foundation for rational development and management of the Huanghe River Delta.

6 CONCLUSION

(1) Sediments above 60 m in the study area consist of Late Pleistocene and Holocene deposits in alternating continental and marine layers. Sediments above 10 m are delta and Holocene neritic deposits with high void ratio, liquidity index and compressibility. Surface sediments are significantly coarser than the underlayer owing to changes in the sedimentary environment after the diversion of the Huanghe River estuary.

(2) On the basis of one-dimensional consolidation theory and calculations at different drilling depth, the final consolidation settlement of each drill hole is between 0.6 m and 2.8 m. Settlement of unit depth generally increases from the surface to the bottom, and the mean settlement of unit depth is 1.5 cm/m to 3.5 cm/m.

(3) The consolidation settlement rate tapers off with time under the condition of no more sediment accumulation. In the first five years, the consolidation degree increases rapidly and can reach 60% to 70%. The consolidation degree needs about 15–20 years to reach 90%. The average sedimentation rate is 5–12 cm/a within 50 m deposition in the study area.

References

- Bie J, Huang H J, Fan H, Bi S P. 2006. Ground subsidence of the modern Yellow River Delta and its causes. *Marine Geology & Quaternary Geology*, **26**(4): 29-35. (in Chinese with English abstract)
- Bie J. 2006. Study and analysis of land subsidence in the Yellow River Delta base on GIS. The Institute of Oceanology, Chinese Academy of Sciences, Qingdao, China. p.3-11. (in Chinese with English abstract)
- Chu Z X, Ma X H, Zhang J Q, Dong M M, Gao Y H. 2005. Comparison of mean high tide line and 2 M isobath reflecting erosion and accretion of the Yellow River delta. *Marine Geology & Quaternary Geology*, **25**(4): 23-27. (in Chinese with English abstract)
- Cui C Q, Shi J T, Zhang Q D. 2001. Modern characteristics of the Ancient Yellow River Delta Coast-Research on the space-time lineage of the Yellow River Delta tidal-flat coast. *Marine Science Bulletin*, **20**(1): 46-52. (in Chinese with English abstract)
- Fan H D, Deng K Z, Ju C Y, Zhu C G, Xue J Q. 2011. Land subsidence monitoring by D-InSAR technique. *Mining Science and Technology (China)*, **21**(6): 869-872.
- Feng X L, Qi H S, Wang T, Li A L, Lin L. 2004. Geomorphological evolution and geological disasters analysis in Chengdao sea area of the Yellow River Delta. *Rock and Soil Mechanics*, **25**(S): 17-20. (in Chinese with English abstract)
- Gili J A, Corominas J, Rius J. 2000. Using global positioning system techniques in landslide monitoring. *Engineering Geology*, **55**(3): 167-192.
- Guan J Y, Gu G C. 2011. Recent erosion characteristics and mechanism of old Yellow River estuarine shoreline. *Coastal engineering*, **30**(2): 50-61. (in Chinese with English abstract)
- Hansbo S. 2003. Deviation from Darcy's law observed in one-dimensional consolidation. *Géotechnique*, **53**(6): 601-605.
- Hu R L, Yue Z Q, Wang L C, Wang S J. 2004. Review on current status and challenging issues of land subsidence in China. *Engineering Geology*, **76**(1-2): 65-77.
- Jiang L M, Lin H. 2010. Integrated analysis of SAR interferometric and geological data for investigating long-term reclamation settlement of Chek Lap Kok Airport, Hong Kong. *Engineering Geology*, **110**(3-4): 77-92.
- Li G G, Hu B Q, Bi J Q, Song Z L, Bu R Y, Li J M. 2013. Stratigraphic evolution of the Huanghe River delta (Bohai Sea) since the Late Quaternary and its paleoenvironmental implications: evidence from core ZK1. *Acta Sedimentologica Sinica*, **31**(6): 1 050-1 058. (in Chinese with English abstract)
- Liu G W, Huang H J, Du T Q, Bie J, Chen J T. 2011. Effective factors of land subsidence in the Yellow River Delta. *Marine Sciences*, **35**(8): 43-50. (in Chinese with English abstract)
- Liu J, Saito Y, Wang H, Zhou L Y, Yang Z G. 2009. Stratigraphic development during the Late Pleistocene and Holocene offshore of the Yellow River delta, Bohai Sea. *Journal of Asian Earth Sciences*, **36**(4-5): 318-331.
- Liu S G, Li C X, Ding J, Li X N, Ivanov V V. 2001. The rough balance of progradation and erosion of the Yellow River delta and its geological meaning. *Marine Geology & Quaternary Geology*, **21**(4): 13-17. (in Chinese with English abstract)
- Liu Y, Li G X, Deng S G, Zhao D B, Wen G Y. 2002. Evolution of erosion and accumulation in the abandoned subaqueous delta lobe of the Yellow River. *Marine Geology & Quaternary Geology*, **22**(3): 27-34. (in Chinese with English abstract)
- Meisina C, Zucca F, Fossati D, Ceriani M, Allievi J. 2006.

- Ground deformation monitoring by using the Permanent Scatterers Technique: the example of the Oltrepo Pavese (Lombardia, Italy). *Engineering Geology*, **88**(3-4): 240-259.
- Miura N, Taesiri Y, Sakai A. 1988. Land subsidence and its influence to geotechnical aspect in Saga plain. In: Proceedings of the International Symposium on Shallow Sea and Lowland. Saga University, Saga, Japan.
- Ortega-Guerrero A, Rudolph D L, Cherry J A. 1999. Analysis of long-term land subsidence near Mexico City: field investigations and predictive modeling. *Water Resources Research*, **35**(11): 3 327-3 341.
- Parcharidis I, Fomelis M, Kourkoulis P, Wegmüller U. 2009. Persistent Scatterers InSAR to detect ground deformation over Rio-Antirio area (Western Greece) for the period 1992-2000. *Journal of Applied Geophysics*, **68**(3): 348-355.
- Qin W Y, Zhuang X G, Huang H J. 2008. Mechanism analysis of land surface subsidence in the modern Yellow River Delta. *Marine Sciences*, **32**(8): 38-43. (in Chinese with English abstract)
- Ren R X Z, Chen S L. 2012. Sediment dynamics in the littoral zone of the Yellow River Delta. *Shanghai Land & Resources*, **33**(2): 62-68. (in Chinese with English abstract)
- Shi C X, Zhang D D, You L Y. 2003. Sediment budget of the Yellow River delta, China: the importance of dry bulk density and implications to understanding of sediment dispersal. *Marine Geology*, **199**(1-2): 13-25.
- Su Y K, Sun X S, Wang L J, Li X L. 2010. Analysis of subsiding on control-points in the Yellow River delta zoom based on GIS methods. *Hydrographic Surveying and Charting*, **30**(5): 32-35. (in Chinese with English abstract)
- Swartzendruber D. 1962. Modification of Darcy's law for the flow of water in soils. *Soil Science*, **93**(1): 22-29.
- Teatini P, Tosi L, Strozzi T, Carbognin L, Wegmüller U, Rizzetto F. 2005. Mapping regional land displacements in the Venice coastland by an integrated monitoring system. *Remote Sensing of Environment*, **98**(4): 403-413.
- Terzaghi K. 1943. Theoretical Soil Mechanics. John Wiley and Son, New York.
- Tung H, Hu J C. 2012. Assessments of serious anthropogenic land subsidence in Yunlin County of central Taiwan from 1996 to 1999 by Persistent Scatterers InSAR. *Tectonophysics*, **578**: 126-135.
- Wang H J, Yang Z S, Li R J, Zhang J, Chang R F. 2001. Numerical modeling of the seabed morphology of the subaqueous Yellow River delta. *International Journal of Sediment Research*, **16**(4): 486-498.
- Wu L X, Gao J H, Ge D Q, Yin Z R, Deng Z Y, Liu H J. 2004. Technical analysis of the remote sensing monitoring for coal-mining subsidence based on D-InSAR. *Geography and Geo-Information Science*, **20**(2): 22-25, 37. (in Chinese with English abstract)
- Xue C T. 1994. Division and recognition of modern Yellow River Delta lobes. *Geographical Research*, **13**(2): 59-66. (in Chinese with English abstract)
- Xue Y Q, Zhang Y, Ye S J, Li Q F. 2003. Land subsidence in China and its problems. *Quaternary Sciences*, **23**(6): 585-593. (in Chinese with English abstract)
- Yang Z S, Keller G H, Lu N Z, Prior D B, Lin T C, Bornhold B D, Xu W D, Wright L D, Suhayda J, Cao L H, Wisenman W J. 1990. Bottom morphology and instability of the modern Huanghe River Subaqueous Delta. *Journal of Ocean University of Qingdao*, **20**(1): 7-21. (in Chinese with English abstract)
- Yellow River Conservancy Commission of MWR. 1951-2012. Annual report of Yellow River sediment bulletin. (in Chinese)
- Zhuang Z Y, Xu W D, Liu D S, Zhuang L H, Liu B Z, Cao Y Y, Wang Q. 1999. Division and environmental evolution of Late Quaternary marine beds of S₃ hole in the Bohai Sea. *Marine Geology & Quaternary Geology*, **19**(2): 27-35. (in Chinese with English abstract)